Photoionization dynamics of glycine adsorbed on a silicon cluster: “On-the-fly” simulations

Dorit Shemesh, Roi Baer, Tamar Seideman, and R. Benny Gerber

Citation: The Journal of Chemical Physics **122**, 184704 (2005);
View online: https://doi.org/10.1063/1.1894052
View Table of Contents: http://aip.scitation.org/toc/jcp/122/18
Published by the American Institute of Physics

HTML ABSTRACT + LINKS

Photoionization dynamics of glycine adsorbed on a silicon cluster: "On-the-fly" simulations

Dorit Shemesh
Department of Physical Chemistry and the Fritz Haber Research Center, The Hebrew University of Jerusalem, Jerusalem 91904, Israel

Roi Baer
Institute of Chemistry and the Lise Meitner Minerva-Center for Quantum Chemistry, The Hebrew University of Jerusalem, Jerusalem 91904, Israel

Tamar Seideman
Department of Chemistry, Northwestern University, Evanston, Illinois 60208-3113

R. Benny Gerber[a)]
Department of Physical Chemistry and the Fritz Haber Research Center, The Hebrew University of Jerusalem, Jerusalem 91904, Israel and Department of Chemistry, University of California, Irvine, California 92697

(Received 28 December 2004; accepted 25 February 2005; published online 9 May 2005)

Dynamics of glycine chemisorbed on the surface of a silicon cluster is studied for a process that involves single-photon ionization, followed by recombination with the electron after a selected time delay. The process is studied by "on-the-fly" molecular dynamics simulations, using the semiempirical parametric method number 3 (PM3) potential energy surface. The system is taken to be in the ground state prior to photoionization, and time delays from 5 to 50 fs before the recombination are considered. The time evolution is computed over 10 ps. The main findings are (1) the positive charge after ionization is initially mostly distributed on the silicon cluster. (2) After ionization the major structural changes are on the silicon cluster. These include Si–Si bond breaking and formation and hydrogen transfer between different silicon atoms. (3) The transient ionization event gives rise to dynamical behavior that depends sensitively on the ion state lifetime. Subsequent to 45 fs evolution in the charged state, the glycine molecule starts to rotate on the silicon cluster. Implications of the results to various processes that are induced by transient transition to a charged state are discussed. These include inelastic tunneling in molecular devices, photochemistry on conducting surfaces, and electron-molecule scattering. © *2005 American Institute of Physics*. [DOI: 10.1063/1.1894052]

I. INTRODUCTION

The adsorption of amino acids on the surfaces of metals and oxides has been attracting much attention for several decades, as it is of great significance for applications such as solid-phase peptide synthesis, development of organic mass spectrometry, medical implants, and biomedical sensors.[1,2] In particular, the adsorption of glycine (and also other amino acids) on different surfaces, e.g., Cu(110), Cu(111), TiO_2, graphite (0001), Silica, Si(100)-2×1 is experimentally and theoretically well studied.[3–11] A related problem of fundamental interest and potential practical benefit is that of nuclear dynamics driven by a transient charging event.[12–30] A rather diverse range of phenomena in molecular dynamics are triggered by an excitation into a short-lived (at least partially) ionic resonance, whose equilibrium configuration differs from that of the initial state. The equilibrium displacement provides a mechanism for channeling of electronic energy into vibrational excitation; upon relaxation to the initial neutral state the vibrational system is internally excited and interesting dynamics is likely to ensue.[26] Examples include the problem of phototriggered, substrate mediated chemistry on conducting surfaces,[18–20,22,24,25] inelastic resonant current and the consequent dynamics in molecular electronics[21,23,26–30] and radiation damage of DNA, to mention but a few of many examples. These processes have been studied theoretically in considerable detail, mostly in the context of desorption induced by electronic transitions.[18,19,22,24,25] To our knowledge, however, studies so far have been limited to cases where the nuclear dynamics is confined to one or two modes. Much richer dynamics is expected (and found below) in truly multidimensional systems, where several modes of comparable time scale are coupled.

Further motivation for the study below comes from the field of photoionization of biological molecules. Little is currently known on the dynamical processes that take place in such events and this certainly applies to molecules adsorbed on surfaces.

In the present paper we address these issues using molecular dynamics simulations and the example of Glycine/Si(100). We focus on single-photon ionization, since this is probably the conceptually simplest ionization process. It

[a)]Author to whom correspondence should be addressed. Electronic mail: benny@fh.huji.ac.il

 © 2005 American Institute of Physics

should be recognized, however, that two- and higher-order photon ionization are far more common in practice. Glycine is adopted here as a prototypical example being the smallest amino acid. The surface is simulated using a silicon cluster built of nine silicon atoms and saturated by hydrogens.[28] It would be interesting to study also larger clusters. However, it should be noted that the cluster used here is an experimentally realistic system by itself, and is not only a representative system for a silicon surface. Also, it is expected that the most interesting changes after ionization will occur near the molecule attached to surface at least for short time scales. Thus we expect the dynamics in larger clusters to be similar to the studied case for short time durations.

The most stable conformer of glycine is attached to a silicon cluster by cleavage of the OH bond (from the carboxylic group) and formation of a Si–O linkage. High-resolution electron energy loss spectroscopy and *ab initio* calculations have shown[10,11] that glycine prefers to bind through the carboxylic group and not through the amino group.

Recently, single-photon ionization dynamics of isolated glycine molecule was studied by classical trajectory simulations using the semiempirical PM3 potential surface in "on-the-fly" calculations.[31] It was shown that the photoionization triggers fast internal rotation about the C–C bond, with the NH_2 group rotating in one direction, and the COOH group rotating in the opposite direction. For the trajectories where fast rotation occurs, it persists until the end of the simulation (10 ps) with a yield of about 2%. Also, for many of the trajectories, the photoproduced glycine ion exhibits "hops" between two conformer structures. The question arises if glycine adsorbed on a surface exhibits the same behavior and how rapidly does the internal excitation dissipates due to the coupling with the substrate. In the gas phase, ionization of glycine leads to a positive charge localized on the nitrogen. It is of interest to know whether this is the case also with glycine adsorbed on the silicon cluster. The channels that open up upon ionization of glycine include: internal flow and redistribution of the vibrational energy between the modes; conformational changes of the nascent ion; transfer of a hydrogen within the ion; fragmentation of the ion. The study presented here focuses mostly on the first two types of processes: intramolecular vibrational energy redistribution and structural changes. These are believed to be the fastest and most efficient dynamical processes in such systems.

The present paper explores the dynamical evolution of the system after ionization and after recombination of the ion with the electron using classical trajectory simulations and a semiempirical potential surface, the choice of which will be discussed later. The structure of the paper is as follows. Section II presents the methodology used, in Sec. III the findings are described and analyzed, and Sec. IV presents concluding remarks.

II. METHODOLOGY

A. The potential energy surface

Our model consists of a glycine molecule connected through the hydroxylic oxygen to a silicon cluster and includes a total of 31 atoms.

Ab initio potentials can be used for this system, but are computationally expensive, due to the dimensionality of the system. In dynamical simulations the potential energy is evaluated thousands of times along the trajectories. This step is the main computational effort and using *ab initio* potentials would be very time consuming. Such *ab initio* simulations would be limited to very short time scales. The present system is an open shell system, which further limits the type of potential that can be used.

Therefore, we use in this study the parametric method number 3 (PM3) semiempirical electronic structure theory.[32,33] PM3 is one of several modified semiempirical NDDO approximation methods.[34] (NDDO—Neglect of diatomic differential overlap) Rather than performing a calculation of all the integrals required in the formation of the Fock Matrix, three- and four-center integrals are neglected in PM3, and one-center, two-electron integrals are parametrized. Thus, in principle, PM3 is closer to *ab initio* methods than force fields. Recently, Shemesh *et al.*[31] have used PM3 to study the photoionization dynamics of isolated glycine. It was shown that PM3 can describe qualitatively well rotational and fragmentation barriers for this system. Although in the case of glycine+ PM3 is able to describe the breaking of bonds, it is not clear to what extent this holds for other systems.

PM3 is applicable to large systems. Recently, PM3 has been applied to calculations of small proteins.[35–37] PM3 can also be improved, as shown by our group in a previous publication,[38] employing a coordinate scaling procedure. The modified PM3 potential has been tested for glycine, alanine, and proline by calculating the anharmonic frequencies using the vibrational self-consistent field method (VSCF) and correlation-corrected vibrational self-consistent field method (CC-VSCF) (Refs. 39 and 40) method, and comparing them to experimental data. The computed anharmonic frequencies are in very good agreement with spectroscopic experiments for these three amino acids. The simulations presented here were carried out with standard PM3. All calculations have been performed using the electronic structure package GAMESS.[41] The most stable conformer of glycine has been attached to a silicon cluster by cleavage of the OH bond (from the carboxylic group) and formation of a Si–O linkage. High-resolution electron energy loss spectroscopy and *ab initio* calculations have shown[10,11] that glycine binds preferentially through the carboxylic group rather than through the amino group. This structure has been optimized by PM3 semiempirical electronic structure theory on the neutral surface. The second derivative (Hessian) matrix was calculated to ensure that the stationary point is indeed a minimum (all eigenvalues are positive). Harmonic normal mode analysis was performed on this geometry. For this geometry ionization was modeled by vertical promotion into the ionic potential energy surface. Subsequently, the trajectory was propagated in time on the ionic PM3 potential energy surface [using restricted open-shell Hartree–Fock method (ROHF) in the Hartree–Fock part of the code] for up to 100 fs. The neutralization was modeled as a vertical transition, conserving the coordinates and momenta in the transformation from the ionic to the neutral surface. The delay time was chosen

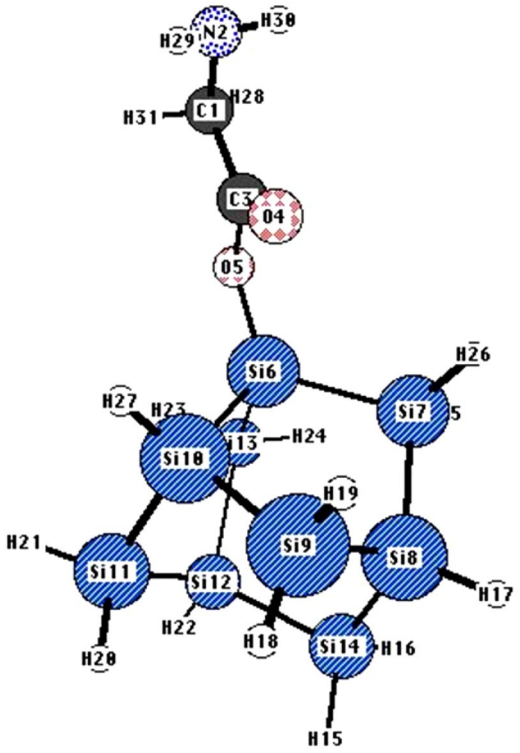

FIG. 1. Initial geometry as calculated by PM3.

between 5 fs and up to 50 fs (in 5 fs steps). On the neutral surface, each trajectory was propagated for another 10 ps. The kinetic energy of each mode in every trajectory was calculated vs time. The system was divided into a subset of normal modes located predominantly on the glycine (21 normal modes) and a subset of modes located predominantly on the cluster. The kinetic energies of the glycine atoms and of the cluster atoms were separately summed and temperatures for the molecule and for the cluster subsets were defined in terms of the corresponding kinetic energies. The temperature of each part at time t is thus

$$T(t) = \frac{2E_{\mathrm{kin}}(t)}{k}, \tag{1}$$

where k is the Boltzmann factor and $E_{\mathrm{kin}}(t)$ is the kinetic energy at time t. The high frequency fluctuations of the effective temperatures were smoothed with respect to time variation. The partial charges on the atoms were evaluated as functions of time following the Coulson definition.[42] (Coulson charges are referred to as MOPAC charges in GAMESS, since the semiempirical potentials in GAMESS originate from the MOPAC6.0 code.[43]

B. On-the-fly molecular dynamics simulation

The simulation was carried using on-the-fly molecular dynamics[44–50] as implemented into the electronic structure program package GAMESS.[41] Recent studies of dynamics on the fly using quantum mechanics/molecular mechanics (QM/MM) and semiempirical potentials have been pursued by Hase[51,52] and co-workers. Quantum effects, neglected in this approach, are expected to play a role, in particular zero-point energy. Given, however, the relatively large excess energy involved in the electron-triggered dynamics, the classical description may be expected to provide a reasonable, although rough approximation. In on-the-fly molecular dynamics, at each time step the potential energy is reevaluated, the forces are updated and the atoms are displaced to their new position. A stringent self-consistent-field (SCF) convergence criterion of 10^{-11} was employed to ensure highly accurate force estimation. This is mandatory for the time scale of the study. We found the default GAMESS value of 10^{-5} to be too large for the present case: calculations using this value produced

TABLE I. MOPAC charges on glycine in the gas phase compared to the MOPAC charges of glycine adsorbed on the silicon cluster.

Atom	Glycine adsorbed on the silicon cluster	Glycine in the gas phase
C 1	−0.0941	−0.1004
N 2	−0.0189	−0.0150
C 3	0.3546	0.3446
O 4	−0.3975	−0.4013
O 5	−0.3950	−0.3016
Si 6	0.3173	
Si 7	0.1508	
Si 8	0.0690	
Si 9	0.1745	
Si10	0.0540	
Si11	0.1656	
Si12	0.0662	
Si13	0.1525	
Si14	0.1745	
H15	−0.0791	
H16	−0.0812	
H17	−0.0782	
H18	−0.0725	
H19	−0.0778	
H20	−0.0724	
H21	−0.0845	
H22	−0.0788	
H23	−0.0878	
H24	−0.0714	
H25	−0.0726	
H26	−0.0818	
H27	−0.0728	
H28	0.0832	0.0869
H29	0.0347	0.0358
H30	0.0354	0.0358
H31	0.0841	0.0869

TABLE II. MOPAC charges on silicon atoms before and after ionization.

Atom	Neutral system	Ionic system
Si 6	0.3173	0.4914
Si 7	0.1508	0.3927
Si 8	0.0690	0.1417
Si 9	0.1745	0.2586
Si10	0.0540	0.0976
Si11	0.1656	0.2630
Si12	0.0662	0.1318
Si13	0.1525	0.3322
Si14	0.1745	0.2333

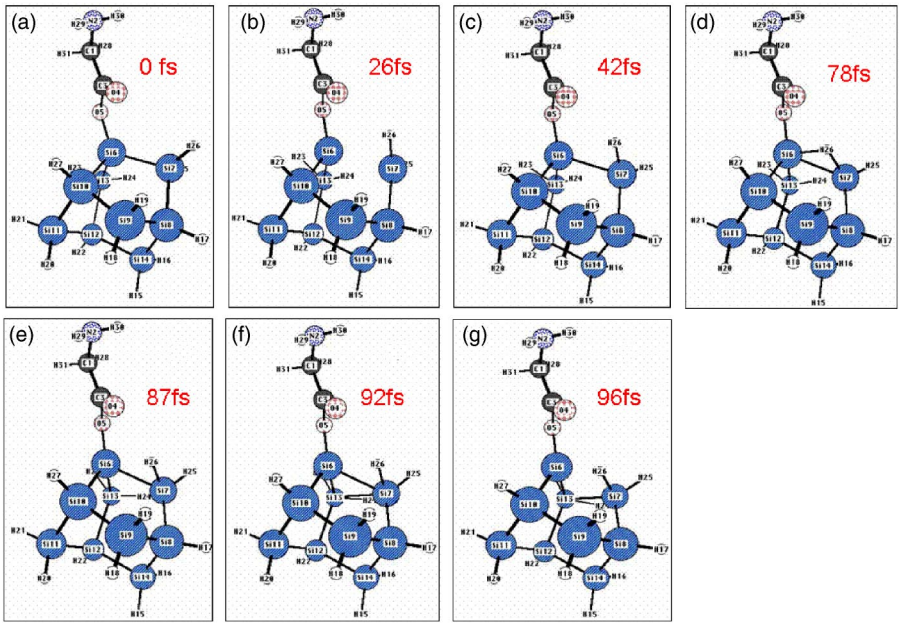

FIG. 2. Snapshots on the dynamics on the ionic surface up to 100 fs.

trajectories containing unphysical artifacts. The reason is obvious: a more accurate potential energy will result in higher quality force. Fewer errors then accumulate during the long-time simulation and the calculated trajectory better conforms to the true one. From our experience, in order to avoid the problem for open shells, the SCF convergence criterion must be more demanding. It seems that for closed shell the standard criterion is fine.

C. Initial conditions

Glycine is chemisorbed on a silicon surface. The surface is simulated using a silicon cluster build of nine silicon atoms and saturated by hydrogens. The most stable conformer of glycine has been attached to a silicon cluster by cleavage of the OH bond (from the carboxylic group) and formation of a Si–O linkage. High-resolution electron energy loss spectroscopy and *ab initio* calculations have shown[10,11] that glycine prefers to bind through the carboxylic group rather than through the amino group. The system is assumed to be initially in its vibrational ground state. This geometry is suddenly, vertically, ionized by a single photon (Franck–Condon approximation). Subsequently, the system is propagated on the ionic ground-state potential surface for up to 100 fs. Recombination is assumed to be fast as well, and the system finds itself back on the neutral ground-state surface, having the position and velocity it acquired on the ionic surface. We study the results as a function of the time delay between ionization and recombination, taken in the interval 5 fs and 50 fs. After recombination, the system is propagated in time for the period of 10 ps, allowing us to study the resulting dynamics.

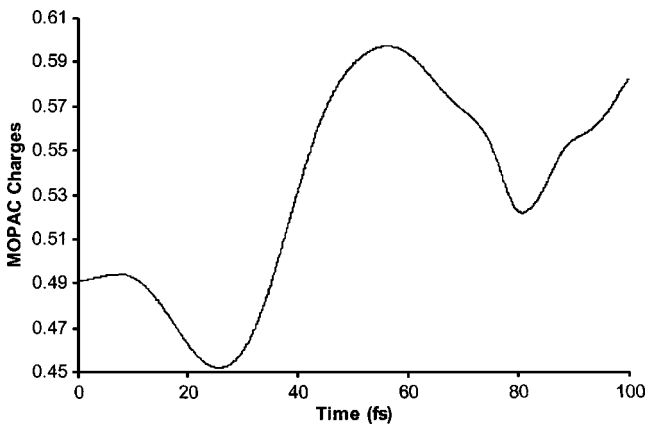

FIG. 3. Charge changes on Si 6 during the dynamics on the ionic surface.

III. RESULTS AND DISCUSSION

A. Initial state

1. Equilibrium geometry of the system

The global equilibrium of the glycine/cluster system is a structure wherein the glycine attaches to the cluster through the carboxylic oxygen and is almost perpendicular to the silicon surface. The initial geometry calculated by PM3 is drawn in Fig. 1. For comparison, this geometry has also been optimized by Hartree–Fock using a double zeta polarisation (DZP) basis set. The geometry is essentially the same with both approaches, with the bond lengths differing by up to 0.03 Å and most of the angles differing by less than 2° (while some differ by up to 8°). It can be concluded, that

TABLE III. Excess energy as a function of the delay time.

Delay time (fs)	Excess energy (eV)
5	0.14
10	0.50
15	0.94
20	1.36
25	1.75
30	2.03
35	2.17
40	2.17
45	2.02
50	1.80

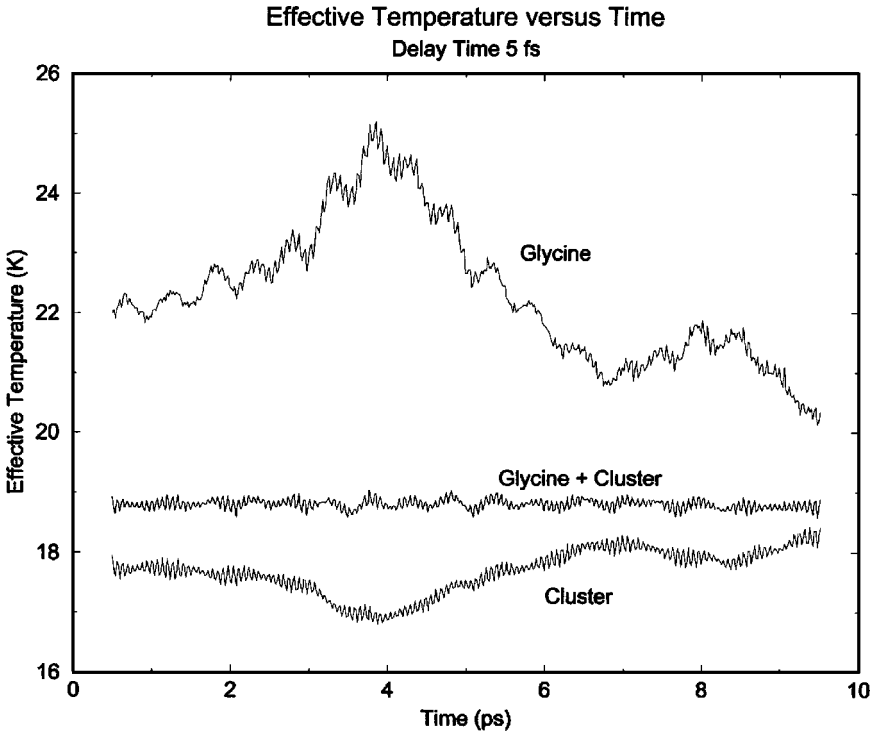

FIG. 4. Effective temperature of glycine, the cluster, and the entire system after a delay time of 5 fs.

PM3 describes the geometry well. Of particular importance is the geometry and bonding of the silicon atoms near the glycine molecule, Si6 that directly binds to the molecule and the three silicon atoms to which it is attached. These atoms play a central role in determining the dynamics on the ionic surface.

2. Charge distribution in the initial state

The charge distribution on the adsorbed atoms is summarized in Table I and compared to the charge distribution in an isolated glycine molecule. In the adsorbed state, glycine carries a positive charge that is mostly distributed on C3 and Si6 (MOPAC charges of 0.35 and 0.32, respectively), which are the atoms near the linkage of the glycine to the silicon cluster. Several silicon atoms, as well as the H atoms on the glycine, carry small positive charges, whereas the negative charge lies mainly on the two oxygen atoms (about -0.40), and to a much lesser extent on most of the hydrogens connected to the silicon atoms. The hydrogens connected to glycine have small positive charges. Comparison with the charge distribution in the isolated molecule (see Table I) il-

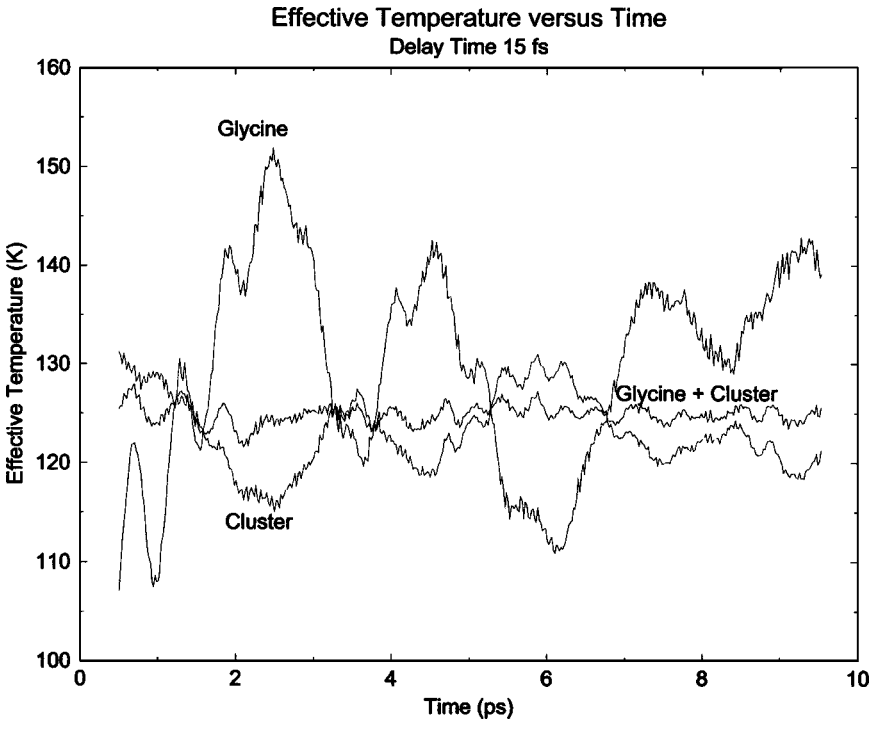

FIG. 5. Effective temperature of glycine, the cluster, and the entire system after a delay time of 15 fs.

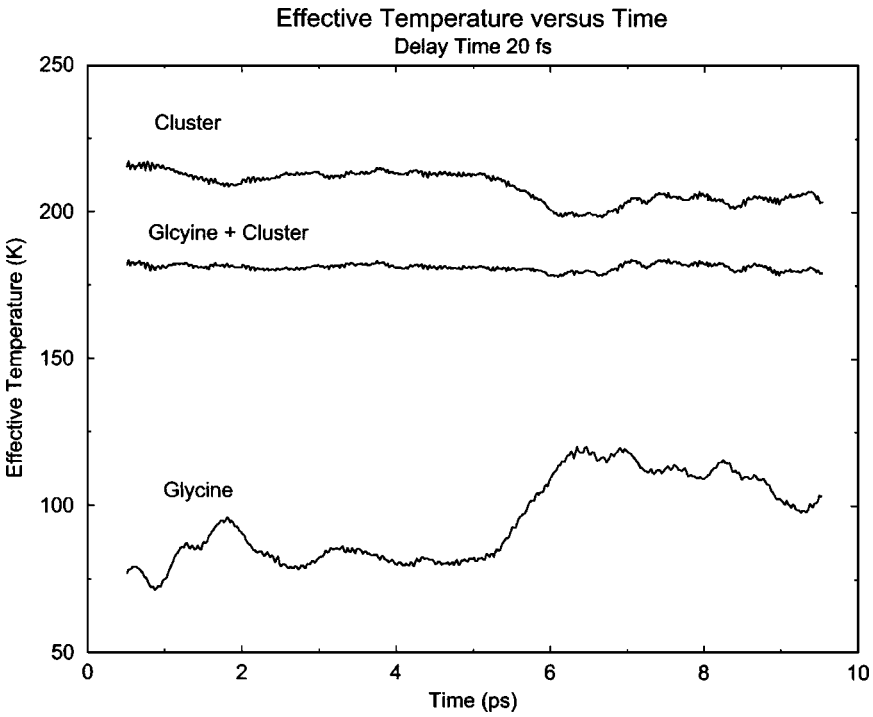

FIG. 6. Effective temperature of glycine, the cluster, and the entire system after a delay time of 5 fs.

lustrates that only minor redistribution of charges occurs upon adsorption, predominantly a reduction of the charge on oxygen 5, which connects the molecule with the cluster, which changes from the isolated molecule charge of -0.3016 to the adsorbed value of -0.3950. The connection of the glycine molecule on the silicon cluster is through this oxygen. The silicon atoms tend to have partial positive charges, therefore the nearby silicon pushes a part of the negative charge to the more electronegative oxygen.

B. Dynamics in the ionic state

1. Charge redistribution upon ionization

Ionization of the glycine molecule in gas phase yields a positive charge, which is mainly located on the nitrogen.[34,53] In contrast, ionization of glycine connected to a silicon cluster yields a positive charge distributed mainly over the silicon atoms. Table II shows the MOPAC charges on the silicon before ionization and after ionization. It can be seen, that the positive charges on all silicon atoms increase upon ionization.

2. Structural changes in glycine due to ionization

Figure 2 shows snapshots of the dynamics on the ionic surface up to 100 fs. It can be seen that the structure of the glycine molecule does not change much upon ionization. The molecule remains perpendicular to the silicon surface and the main changes are on Si6, the silicon atom directly bonded to glycine. The structural changes of the silicon cluster are discussed below.

3. Structural changes of the cluster during the dynamics: Hydrogen transfer, Si–Si bond breaking and formation of new bonds

During the evolution on the ionic surface, the cluster undergoes substantial structural changes, as illustrated in

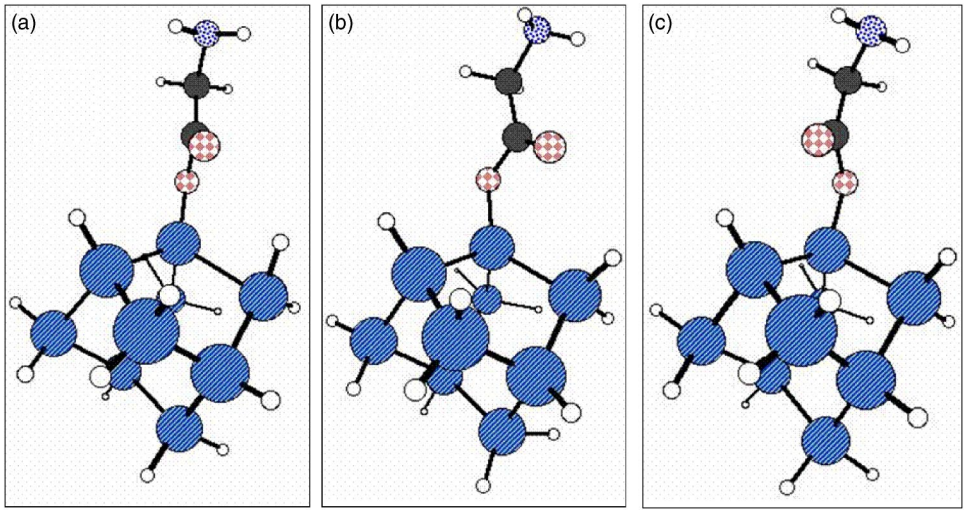

FIG. 7. Torsional motion of the COO group against the CH_2NH_2 group.

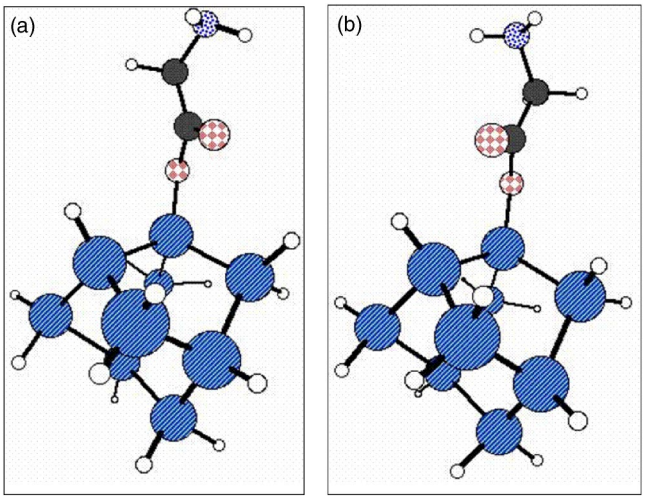

FIG. 8. Rotation of the glycine molecule on the silicon cluster.

Fig. 2. Initially, the Si6–Si7 bond length is 2.40 Å. At 26 fs the bond almost breaks as the distance between the two atoms reaches 2.6 Å. At 42 fs the bond between the atoms is reestablished.

The H26–Si6 distance is initially 3.3 Å. As time progresses, this distance shortens to 1.6 Å and a new bond is formed, with which the H atom has been transferred to Si6 while maintaining bonding character with Si7. At 87 fs this newly formed bond breaks again. Simultaneously, the Si13–Si7 distance falls from 3.6 Å, to 2.4 Å, the typical length of a Si–Si bond in this system. At 96 fs the bond between Si6 and Si7 breaks.

4. Charge changes during the dynamics

The structural changes are accompanied by sharp charge fluctuations on the involved atoms. Si6, which undergoes the main structural changes, also shows strong fluctuations in the positive charge located on it as is shown in Fig. 3. Immediately after ionization, it bears a large amount of positive charge (0.49). This charge decreases until it reaches a minimum at 26 fs, where the Si6–Si7 bond breaks. After that, the positive charge increases again until it reaches a maximum at 56 fs (0.60).

C. Dynamics in the neutral state after recombination

1. Effects of the structural and charge changes during the ionization on the dynamics on the neutral potential energy surface

The neutralization of the newly formed ion is modeled as a Frank–Condon transition, conserving coordinates and momenta, from the ionic to the neutral state subsequent to a variable residence time in the ionic state. The time delay for neutralization in the ionic state is varied between 5 and 50 fs (in 5 fs steps). These are experimentally realistic times. In principle, longer residence times of the system in the ionic state can be also investigated. We will focus here on short residence times. The longer the residence time the larger the displacement of the system from the neutral state equilibrium upon neutralization. Using longer delay times will only give rise to stronger effects but we do not expect new trends. The dominant attribute that determines the dynamics the follows the relaxation is the excess energy, defined as the difference between the total energy upon neutralization and the total energy of the initial state. Table III summarizes the excess energy as a function of the residence time. At short times the excess energy increases with time, since the extent of structural deformation increases with the duration of the ionic state evolution time. The dominating mode in the neutral state dynamics is the Si6–Si7 vibration, with a period of 26 fs. Consequently, for ionic state residence time exceeding 40 fs the excess energy decreases. This large excess energy plays a major role in determining the subsequent dynamics.

2. Effective temperatures of glycine and silicon cluster

The amount of excess energy upon recombination and hence also effective temperature depend on the time delay. Several trajectories with different delay times are selected here to show the different types of dynamics that can emerge following neutralization. Figure 4 shows the effective temperatures of glycine, the cluster and the entire system after 5 fs evolution in the ionic state. For this trajectory, glycine is slightly hotter than the silicon cluster, but the displacement from the initial configuration is too small to induce significant motion. Figure 5 shows the effective temperature of glycine, the silicon cluster, and the whole system after a delay time of 15 fs. Here, at the beginning, the cluster is hotter than glycine, but during the simulation there is an extensive energy flow between the cluster and the glycine. The glycine molecule is sometimes hotter, sometimes colder than the cluster. At this time, both glycine and the cluster have undergone significant structural changes, resulting in energy flow between the system subcomponents. For all the trajectories with delay time higher than 15 fs (i.e., 20, 25, 30, 35, 40, 45, 50) the qualitative picture is the same (see Fig. 6): The cluster is initially hotter than the glycine. During the simulation, glycine gets hotter and the cluster gets colder. The cluster is more distorted from equilibrium than glycine for these delay times and hence the silicon atoms evolve faster than the atoms of the glycine molecule in order to return to the equilibrium configuration. The nearer the cluster gets to its equilibrium geometry, the more energy it loses to glycine and the larger the amplitude of motion within the glycine becomes. Two main movements can be seen in glycine: Figure 7 shows the movement of the COO group in one direction, and the CH_2NH_2 into the other direction. Figure 8 shows the motion of the glycine molecule as a whole on the silicon cluster. This motion can be seen in all trajectories with delay time of at least 20 fs. The most interesting trajectory is the one with the delay time of 45 fs. This trajectory shows the glycine molecule rotating on the cluster, as can be seen in snapshots in Fig. 9. The molecule completes 1.5 revolutions and then stops rotating at 8.8 ps.

In summary, short delay times result in hot glycine and cold cluster. The reason is that glycine is more floppy than the cluster, and therefore undergoes more changes in a short timescale. After a certain delay time (15 fs) the cluster also has undergone structural changes like Si–Si bond breaking and forming and hydrogen transfer. Therefore it deviates

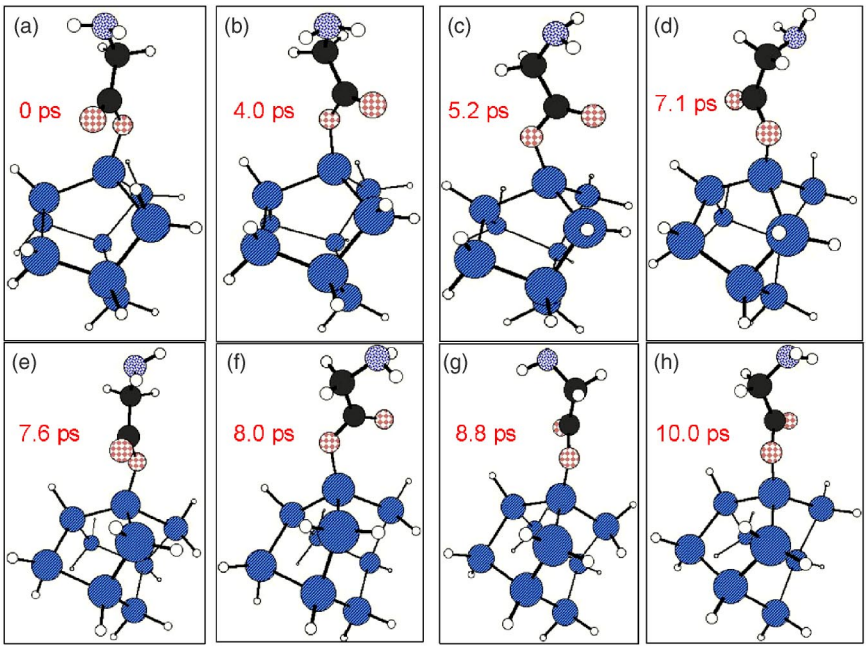

FIG. 9. Snapshot of the rotation of glycine on the silicon cluster.

from the initial equilibrium geometry. After the recombination this results in higher effective temperature of the cluster than of glycine.

3. Final temperature dependence on the delay time

Figure 10 shows the final temperature as a function of the delay time. For small delay times (up to 15 fs), the final temperatures of the glycine and the silicon cluster are almost the same. The system is at equilibrium after 10 ps. For these short delay times, the structure of the system does not change much on the ionic surface, and the system is able to quickly equilibrate after recombination.

For large delay times (greater than 20 fs), the glycine molecule is always colder than the cluster, due to the large changes that the cluster undergoes on the ionic surface. This results in large amplitude displacements upon recombination on the neutral surface leading to high temperatures.

IV. CONCLUDING REMARKS

Single-photon ionization dynamics of glycine adsorbed on a silicon cluster has been studied by classical trajectory simulations using the semiempirical PM3 potential surface in on-the-fly calculations. The ionization yields a positive charge which is distributed on several of the silicon atoms. Structural changes after ionization includes breaking and forming of Si–Si bonds and hydrogen transfer. The dynamics after recombination between the electron and the ion have been modeled for different delay times between the ionization and neutralization events, corresponding to different excess energy available in the system. The largest excess energy is found for a delay time of 40 fs. For trajectories with delay times higher than 15 fs the cluster has a higher effective temperature than glycine. The reason for this behavior is that the cluster has undergone large structural changes and, upon recombination, is subject to strong restoring forces toward the equilibrium configuration. The most interesting finding is the rotation of the glycine molecule on the cluster for a delay time of 45 fs.

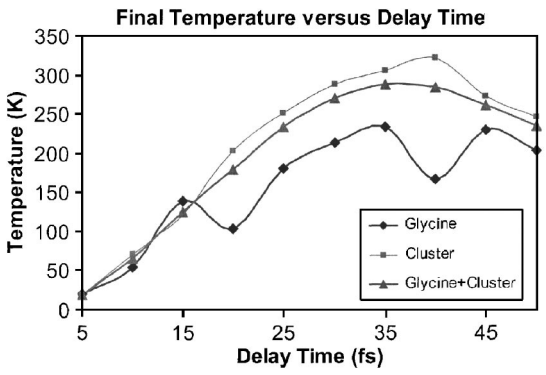

FIG. 10. Final temperatures as a function of the delay time.

ACKNOWLEDGMENT

This research was supported in the framework of the Saerree K. and Louis P. Fiedler Chair in Chemistry.

[1]B. Kasemo, Surf. Sci. **500**, 656 (2002).
[2]W. Langel and L. Menken, Surf. Sci. **538**, 1 (2003).
[3]J. Lausmaa, P. Lofgren, and B. Kasemo, J. Biomed. Mater. Res. **44**, 227 (1999).
[4]R. B. Rankin and D. S. Sholl, Surf. Sci. **548**, 301 (2004).
[5]V. Efstathiou and D. P. Woodruff, Surf. Sci. **531**, 304 (2003).
[6]S. M. Barlow, K. J. Kitching, S. Haq, and N. V. Richardson, Surf. Sci. **401**, 322 (1998).
[7]M. Nyberg, M. Odelius, A. Nilsson, and L. G. M. Petterson, J. Chem. Phys. **119**, 12577 (2003).
[8]P. Lofgren, A. Krozer, D. V. Chakarov, and B. Kasemo, J. Vac. Sci. Technol. A **16**, 2961 (1998).
[9]M. Meng, L. Stievano, and J. F. Lambert, Langmuir **20**, 914 (2004).
[10]A. Lopez, T. Heller, T. Bitzer, and N. V. Richardson, Chem. Phys. **277**, 1 (2002).
[11]Y. Q. Qu, Y. Wang, J. Li, and K. L. Han, Surf. Sci. **569**, 12 (2004).
[12]P. Tran, B. Alavi, and G. Gruner, Phys. Rev. Lett. **85**, 1564 (2000).
[13]M. A. Reed, C. Zhou, C. J. Muller, T. P. Burgin, and J. M. Tour, Science **278**, 252 (1997).
[14]D. Porath, A. Bezryadin, S. de Vries, and C. Dekker, Nature (London)

403, 635 (2000).
[15]V. J. Langlais, R. R. Schlittler, H. Tang, A. Gourdon, C. Joachim, and J. K. Gimzewski, Phys. Rev. Lett. **83**, 2809 (1999).
[16]S. J. Tans, M. H. Devoret, H. J. Dai, A. Thess, R. E. Smalley, L. J. Geerligs, and C. Dekker, Nature (London) **386**, 474 (1997).
[17]M. Magoga and C. Joachim, Phys. Rev. B **56**, 4722 (1997).
[18]J. W. Gadzuk, Surf. Sci. **342**, 345 (1995).
[19]J. W. Gadzuk, Annu. Rev. Phys. Chem. **39**, 395 (1988).
[20]J. W. Gadzuk, Phys. Rev. B **44**, 13466 (1991).
[21]T. Seideman and H. Guo, J. Theor. Comput. Chem. **2**, 439 (2003).
[22]H. Guo, P. Saalfrank, and T. Seideman, Prog. Surf. Sci. **62**, 239 (1999).
[23]S. Alavi, B. Larade, J. Taylor, H. Guo, and T. Seideman, Chem. Phys. **281**, 293 (2002).
[24]D. Menzel and R. Gomer, J. Chem. Phys. **41**, 3311 (1964).
[25]P. A. Redhead, Can. J. Phys. **64**, 886 (1964).
[26]T. Seideman, J. Phys.: Condens. Matter **15**, R521 (2003).
[27]S. Alavi and T. Seideman, J. Chem. Phys. **115**, 1882 (2001).
[28]S. Alavi, R. Rousseau, and T. Seideman, J. Chem. Phys. **113**, 4412 (2000).
[29]S. Alavi, R. Rousseau, S. N. Patitsas, G. P. Lopinski, R. A. Wolkow, and T. Seideman, Phys. Rev. Lett. **85**, 5372 (2000).
[30]S. Alavi, R. Rousseau, G. P. Lopinski, R. A. Wolkow, and T. Seideman, Faraday Discuss. **117**, 213 (2000).
[31]D. Shemesh, G. M. Chaban, and R. B. Gerber, J. Phys. Chem. A **108**, 11477 (2004).
[32]J. J. P. Stewart, J. Comput. Chem. **10**, 209 (1989).
[33]J. J. P. Stewart, J. Comput. Chem. **10**, 221 (1989).
[34]F. Jensen, *Introduction to Computational Chemistry* (Wiley, Chichester, 1999).
[35]J. J. P. Stewart, J. Mol. Struct.: THEOCHEM **401**, 195 (1997).
[36]T. S. Lee, D. M. York, and W. T. Yang, J. Chem. Phys. **105**, 2744 (1996).
[37]A. D. Daniels and G. E. Scuseria, J. Chem. Phys. **110**, 1321 (1999).
[38]B. Brauer, G. M. Chaban, and R. B. Gerber, Phys. Chem. Chem. Phys. **6**, 2543 (2004).
[39]J. O. Jung and R. B. Gerber, J. Chem. Phys. **105**, 10332 (1996).
[40]G. M. Chaban, J. O. Jung, and R. B. Gerber, J. Chem. Phys. **111**, 1823 (1999).
[41]http://www.msg.ameslab.gov/GAMESS/GAMESS.html
[42]B. H. Chirgwin and C. A. Coulson, Proc. R. Soc. London **A201**, 196 (1950).
[43]J. J. P. Stewart, MOPAC, A general molecular orbital package (version 6.0); Quant. Chem. Prog. Exch. 9, 455 (1990).
[44]J. J. P. Stewart, L. P. Davis, and L. W. Burggraf, J. Comput. Chem. **8**, 1117 (1987).
[45]S. A. Maluendes and M. Dupuis, J. Chem. Phys. **93**, 5902 (1990).
[46]M. S. Gordon, G. Chaban, and T. Taketsugu, J. Phys. Chem. **100**, 11512 (1996).
[47]I. Takata, T. Taketsugu, K. Hirao, and M. S. Gordon, J. Chem. Phys. **109**, 4281 (1998).
[48]T. Taketsugu and M. S. Gordon, J. Chem. Phys. **103**, 10042 (1995).
[49]T. Taketsugu and M. S. Gordon, J. Phys. Chem. **99**, 14597 (1995).
[50]T. Taketsugu and M. S. Gordon, J. Phys. Chem. **99**, 8462 (1995).
[51]J. P. Wang, S. O. Meroueh, Y. F. Wang, and W. L. Hase, Int. J. Mass. Spectrom. **230**, 57 (2003).
[52]Y. F. Wang and W. L. Hase, J. Am. Soc. Mass Spectrom. **14**, 1402 (2003).
[53]V. Vorsa, T. Kono, K. F. Willey, and N. Winograd, J. Phys. Chem. B **103**, 7889 (1999).